Journal of Chromatography A, 1217 (2010) 1354–1361

Contents lists available at ScienceDirect

Journal of Chromatography A

journal homepage: www.elsevier.com/locate/chroma

Intermittent simulated moving bed chromatography: 1. Design criteria and cyclic steady-state

Shigeharu Katsuo [1], Marco Mazzotti *

Institute of Process Engineering, ETH Zurich, Sonneggstrasse 3, CH-8092 Zurich, Switzerland

ARTICLE INFO

Article history:
Received 13 October 2009
Received in revised form 7 December 2009
Accepted 22 December 2009
Available online 4 January 2010

Keywords:
Simulated moving bed chromatography
I-SMB
Equilibrium theory

ABSTRACT

The intermittent SMB (I-SMB) process is a multi-column chromatographic process, which is a modification of the conventional SMB process, has been applied so far only in the sugar industry and is claimed to achieve higher productivity. In the I-SMB process the time interval between two port switches is divided in two sub-intervals, and only during the first the product streams are collected. The potential of the I-SMB technology is demonstrated in the case of the separation of a binary mixture subject to the linear isotherm by using both the equilibrium theory of chromatography and detailed simulations. It is shown that a I-SMB with only four columns can achieve much higher separation performance than a SMB unit with four columns.

1. Introduction

The application of simulated moving bed (SMB) chromatography to the separation of enantiomers of chiral compounds is successful because of its excellent performance as compared to column chromatography [1] and of the ease of scaling it, both up and down. Since chiral stationary phases can be relatively expensive compared to others, there has been a continuous effort to find modified SMB schemes that allow for higher productivity or for a smaller number of columns yet guaranteeing the same product specifications [2]. Examples of such modifications are the processes called Varicol, where the ports are switched asynchronously [3], ModiCon, where the feed concentration is modulated during the switch interval [4], PowerFeed, where the feed flow rate is varied [5], and FF-SMB, where the product stream is fractionated for internal re-cycling and re-feeding [6].

In this study, one of such modifications is presented and analyzed in the frame of the equilibrium theory of chromatography and through detailed simulations. This process was invented and patented under the name of improved SMB by Nippon Rensui Corporation, and uses typically only four chromatographic columns [7]. The proponents claim that higher productivity than in the conventional SMB can be achieved, and they have applied it for separations in the sugar industry.

We prefer to call this new process intermittent SMB (I-SMB) because this name reflects better its features, as we will see in the following. In this first part of a series of papers, Triangle Theory as developed for the conventional SMB [8,9] is extended to the I-SMB process design. Additionally, through the equilibrium theory-based cyclic steady-state analysis, the benefits of this process are discussed and it is demonstrated why and how the combination of the synchronous partial feed and partial withdrawal operation implemented in the I-SMB process can indeed improve the separation efficiency as compared to the standard SMB process. In the next papers of the series experimental evidence of the I-SMB performance under linear and nonlinear conditions will be provided, and results about the I-SMB optimization will be reported.

2. I-SMB chromatography

2.1. Process description

Fig. 1 shows the scheme of the conventional closed-loop SMB process. A series of columns is divided into four zones by two inlet and two outlet ports. The feed solution and the mobile phase are introduced through the inlet ports (feed and desorbent) and the two product streams are withdrawn from the outlet ports (extract and raffinate) continuously. Periodically the port locations are switched in the direction of the fluid flow, thus simulating in a discrete manner a continuous counter-current movement of the stationary phase with respect to the fluid phase.

In the I-SMB process however, as illustrated in Fig. 2(a), the time period between two port switches, t^*, is divided into two

* Corresponding author. Tel.: +41 44 632 24 56; fax: +41 44 632 11 41.
E-mail address: marco.mazzotti@ipe.mavt.ethz.ch (M. Mazzotti).
[1] Permanent address: Mitsubishi Chemical Group Science and Technology Research Center., Inc., 1000, Kamoshida-cho, Aoba-ku, Yokohama 227-8502, Japan.

0021-9673/$ – see front matter © 2010 Elsevier B.V. All rights reserved.
doi:10.1016/j.chroma.2009.12.065

Nomenclature

c_i	fluid phase concentration of component i
D_i	axial dispersion coefficient of component i
H_i	Henry constant of component i
$k_{s,i}a_v$	mass transfer coefficient of component i
L	column length
m_j	flow rate ratio in section j of I-SMB and conventional SMB
n_i^*	adsorbed phase concentration of component i in equilibrium with the mobile phase
n_j	number of the columns in section j
ΔP_j	pressure drop in section j
Q_j	volumetric flow rate in section j
$\hat{Q}_j$	average volumetric flow rate in section j
Q_P	volumetric flow rate at port P
S	cross-sectional area of the column
t	time coordinate
t^*	switch time
$t_{i,j}^r$	retention time of component i in section j
u	superficial velocity
v_i	propagation velocity of component i
V	column volume
z	axial coordinate along the column

Greek letters

α	step ratio of I-SMB
ϵ^*	overall bed void fraction
ϵ_b	inter-particle void fraction
ϕ	pressure drop coefficient in Eq. (9)

Subscripts and superscripts

A	component A
B	component B
i	component index
j	section index

sub-intervals, namely steps I and II, with duration αt^* and $(1-\alpha)t^*$, respectively. During step I, the unit is operated as a conventional SMB, with two inlets and two outlets, though with zero flow rate in Section 4 (Fig. 2(b)). During step II all the inlet and outlet ports are closed hence the fluid phase is just circulated along the column train, with identical flow rates in the four sections, thus allowing to move the concentration profiles along the columns and to adjust their relative position with respect to the location of the inlet and outlet ports (Fig. 2(c)). Since there is flow in Section 4 during step II only, we call the corresponding flow rate Q_4, and the three flow rates in Sections 1–3, which prevail during step I, are called Q_1, Q_2 and Q_3, respectively. Note that only three sections are used during step I in order to reduce the overall length of the unit and to allow for larger flow rates in the columns at the same overall pressure drop, as discussed below. Note also that the choice of having the same flow rate in all sections during step II makes the implementation of the I-SMB mode rather simple.

2.2. Triangle Theory for I-SMB

For the sake of simplicity, let us consider two components A and B subject to a linear adsorption isotherm:

$$\begin{aligned} &n_i^* = H_i c_i \quad (i = \mathrm{A,B}),\\ &H_\mathrm{A} > H_\mathrm{B}, \end{aligned} \tag{1}$$

where for each component i H_i is its Henry's constant, whereas c_i is its concentration in the fluid phase and n_i^* is its adsorbed phase concentration in equilibrium with the fluid phase.

Like in the case of the conventional SMB [10,2], also in the case of the I-SMB under the assumption of infinite column efficiency the constraints to achieve complete separation in sections 2 and 3 and to achieve complete regeneration of the stationary and mobile phase in sections 1 and 4 can be expressed in terms of the residence time of the two components to be separated in each section of the unit:

$$\begin{aligned} &\text{Section 1}: \quad t_{\mathrm{A},1}^r \le t^*,\\ &\text{Section 2}: \quad t_{\mathrm{B},2}^r \le t^* \le t_{\mathrm{A},2}^r,\\ &\text{Section 3}: \quad t_{\mathrm{B},3}^r \le t^* \le t_{\mathrm{A},3}^r,\\ &\text{Section 4}: \quad t^* \le t_{\mathrm{B},4}^r. \end{aligned} \tag{2}$$

Taking into account that each I-SMB section experiences two different flow rates during each switch period t^*, the retention time of species i in the j-th section $t_{i,j}^r$ is given by the following equation:

$$t_{i,j}^r = \frac{V}{\hat{Q}_j}[\epsilon^* + (1-\epsilon^*)H_i] \quad (i = \mathrm{A,B}, \quad j = 1,\ldots,4), \tag{3}$$

where V and ϵ^* are the column volume and overall void fraction, respectively, whereas $\hat{Q}_j$ is the flow rate in the j-th section averaged over one switch period. This is defined as

$$\begin{aligned} &\hat{Q}_j = \alpha Q_j + (1-\alpha)Q_4, \quad (j = 1,2,3),\\ &\hat{Q}_4 = (1-\alpha)Q_4. \end{aligned} \tag{4}$$

It is worth noting that Eq. (3) applies also to the conventional SMB when the actual flow rates are used for the average flow rates, i.e. where $\hat{Q}_j = Q_j$. Let us introduce the flow rate ratio m_j defined using the average flow rate, i.e.:

$$m_j \equiv \frac{\hat{Q}_j t^* - V\epsilon^*}{V(1-\epsilon^*)} \quad (j = 1,\ldots,4). \tag{5}$$

Note that this definition applies also to the conventional SMB when $\hat{Q}_j = Q_j$. By using Eq. (3), the inequalities on the retention times given by Eq. (2) can be readily recast in terms of the flow rate ratios as follows:

$$\begin{aligned} H_\mathrm{A} \le\ & m_1,\\ H_\mathrm{B} \le\ & m_2 \le H_\mathrm{A},\\ H_\mathrm{B} \le\ & m_3 \le H_\mathrm{A},\\ & m_4 \le H_\mathrm{B}. \end{aligned} \tag{6}$$

This demonstrates that at least in the case of linear systems, I-SMB operating conditions can be selected using the same criteria in terms of the flow rate ratios m_j as those applied in the case of the conventional SMB operation.

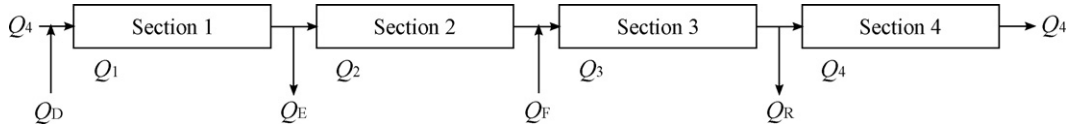

Fig. 1. Scheme of the conventional closed-loop SMB process.

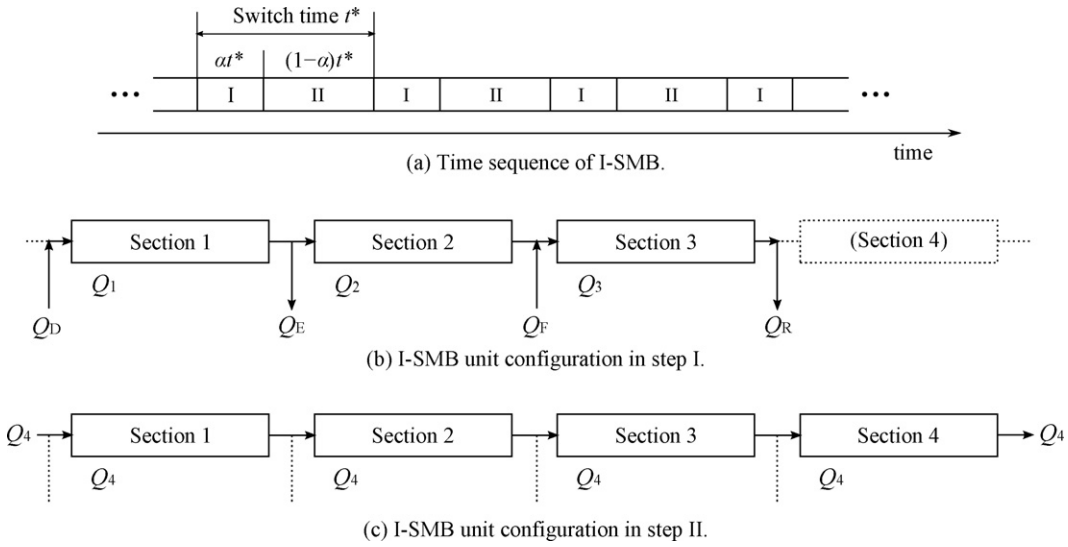

Fig. 2. Scheme of the I-SMB process and definition of the flow rates. Port switch takes place at the end of step II and at the start of step I.

Based on the process schemes in Figs. 1 and 2, it is obvious that the external flow rates can be obtained from the internal flow rates differently for the two units, as given by the following equations:

$$\begin{aligned} &Q_E = Q_1 - Q_2, \\ &Q_F = Q_3 - Q_2, \\ &Q_D = Q_1 \quad \text{(I-SMB)}, \\ &Q_R = Q_3 \quad \text{(I-SMB)}, \\ &Q_D = Q_1 - Q_4 \quad \text{(SMB)}, \\ &Q_R = Q_3 - Q_4 \quad \text{(SMB)}. \end{aligned} \tag{7}$$

Using these equations and the requirement of non-negativity for both internal and external flow rates yields the following additional constraints:

$$\begin{aligned} &m_j \geq m_2 \geq m_4 \geq \frac{-\epsilon^*}{1-\epsilon^*} \quad (j = 1, 3) \quad \text{(I-SMB)}, \\ &m_j \geq m_k \geq \frac{-\epsilon^*}{1-\epsilon^*} \quad (j = 1, 3;\ k = 2, 4) \quad \text{(SMB)}. \end{aligned} \tag{8}$$

An example of the complete separation triangle for the I-SMB and the conventional SMB processes is shown in Fig. 3.

2.3. Minimum switch time design

The I-SMB process has six degrees of freedom, namely the four internal flow rates Q_j ($j = 1, \ldots, 4$), the switch time t^* and the parameter α, which defines the duration of sub-interval I relative to the whole switch time t^*. To determine the values of these six operating parameters, the constraints on the four m_j values provided above (Eq. (6)) and two additional constraints need to be enforced.

Typically the chromatographic media, particularly for chiral separations, have a specification on the maximum pressure drop, ΔP_{max}, i.e. violating this maximum allowable pressure drop would damage the stationary phase and consequently lead to degradation of the separation performance. Therefore, for conventional SMBs, and for I-SMBs as well, the additional constraints to determine the operating conditions require that the total pressure drop in the unit be smaller than or equal to the maximum pressure drop. This is particularly true for highly efficient stationary phases, such as chiral stationary phases, where efficiency limitations are less stringent than pressure drop limitations. Therefore, in the following we assume that pressure drop is the limiting constraint.

The pressure drop ΔP_j along one column in section j associated to the fluid flow rate Q_j is given by Darcy's law as:

$$\frac{\Delta P_j}{L} = \frac{\phi Q_j}{S}, \tag{9}$$

where L and S are the column length and cross-sectional area, respectively, and ϕ is a parameter depending on the properties of the packing and of the fluid phase. In the case of multicolumn chromatographic processes, since the flow rates differ in different sections, the total pressure drop ΔP in the unit must be expressed as the summation of each section's pressure drops, i.e.:

$$\Delta P = \sum_j n_j \Delta P_j \tag{10}$$

where n_j is the number of columns in the j-th section of the unit.

Since the I-SMB experiences two different operating modes during one switch period and the pressure drop constraint applies to

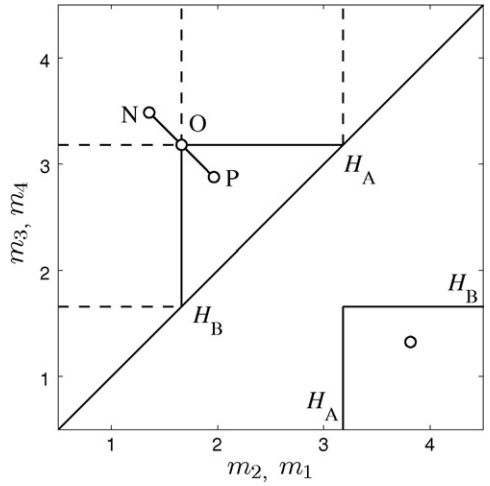

Fig. 3. Complete separation and regeneration region for the I-SMB process. Open symbols represent operating points for the cyclic steady-state analysis. Point P: inside the complete separation region. Point O: at the triangle vertex. Point N: in the region where both product streams are impure. Simulations have been carried out for all operating points connecting points N and P. The values of m_1 and m_4 are the same for all cases.

both, the following inequalities have to be fulfilled:

$$\Delta P_{\mathrm{I}} = \sum_{j=1}^{3} n_j \Delta P_j \le \Delta P_{\max} \quad \text{for sub-interval I,}$$
$$\Delta P_{\mathrm{II}} = \sum_{j=1}^{4} n_j \Delta P_4 \le \Delta P_{\max} \quad \text{for sub-interval II.} \tag{11}$$

With a given set of four m_j values, the condition $\Delta P_{\mathrm{I}} = \Delta P_{\mathrm{II}} = \Delta P_{\max}$ allows calculating the minimum switch time t^* and the parameter α, which therefore gives the minimum duration of step I. Using Eqs. (5), (9) and (11), the following relationships are obtained:

$$t^* = \frac{\phi L^2}{\Delta P_{\max}} \sum_{j=1}^{4} n_j (m_j(1-\epsilon^*) + \epsilon^*), \tag{12}$$

$$\alpha = \frac{\sum_{j=1}^{3} n_j (m_j - m_4)(1-\epsilon^*)}{\sum_{j=1}^{4} n_j (m_j(1-\epsilon^*) + \epsilon^*)}. \tag{13}$$

It is worth noting that the expression of the minimum switch time applies also to the conventional SMB operated at the same m_j values, where only one of the two constraints given by Eq. (11) applies. Remarkably, t^* and α are independent of each other. For given I-SMB unit and conventional SMB unit having the same geometric configuration, if the same flow rate ratio values and pressure drop constraints are applied when designing the process, the switch time of both processes is the same and the average flow rate in each section of the I-SMB is equal to that of the standard SMB. This implies that the two units achieve the same throughput, i.e. the same amount of feed processed per unit time, when operated at the same feed concentration. Therefore, the I-SMB and the conventional SMB processes can be conveniently compared on the same basis by considering the corresponding flow rate ratios.

3. Analysis of the cyclic steady-state behavior

We aim at comparing the cyclic steady-state behavior of the conventional SMB process and of the I-SMB process in terms of separation performance. On the one hand we consider for the two techniques operating points sharing the same values of the flow rate ratios, hence, based on the considerations above, the same throughput. On the other hand, the productivity of the process is defined as the amount of product recovered per unit time and per unit volume of the stationary phase (or of the unit) that fulfill the product specifications, typically the average product purities [1]. Therefore, the same throughput in two different units corresponds to the same productivity only if the units have the same total volume, or more specifically the same number of columns of the same size, and if the same product purities are achieved.

Let us consider the graphical representation of the complete separation region defined by Eqs. (6) and (8) in the m_2-m_3 plane as shown in Fig. 3. For a given value of the flow rate ratios in sections 1 and 4 and for a fixed value of the switch time t^*, the vertex of the complete separation triangle (point O in the figure) achieves the highest throughput, i.e. the feed flow rate $Q_F = Q_3 - Q_2$ is maximized, among the operating points belonging to the complete separation region.

However, the complete separation region has been obtained assuming columns with infinite efficiency. Therefore in the operation of real columns with finite efficiency, due to mass transfer resistance and axial dispersion, and in detailed simulations that account for these effects, the separation does not reach very high product purity in the neighborhood of the triangle's vertex. This is particularly true for a conventional four column SMB with 1-1-1-1 configuration (one column per section, like in Fig. 1). Typically SMB units have in fact six or more columns to overcome this limitation. On the contrary the patent literature claims that a four-column I-SMB unit is not affected by such purity limitations, thus reaching much higher productivity than a conventional SMB [7]. We will address this issue in detail in the following by carrying out a theoretical analysis based on equilibrium theory supported by detailed simulations.

Table 1
Column and system parameters [11].

Column		
S (cm^2)	0.166	
L (cm)	15.0	
ϵ^*	0.63	
$\Delta P_{\max}$ (bar)	40	
System characteristics	**Component**	
	A	B
Isotherm	Linear	
H_i	3.18	1.66
$k_{s,i}a_v$ (1/s) [a]	1.82	2.70
$\epsilon_b D_{ax,i}/u$ (m) [b]	2.21×10^{-5}	
ϕ (bar min/cm^2) [c]	0.0196	

[a] Product of mass transfer coefficient and specific surface.
[b] Coefficient to determine the dispersion coefficient, where ϵ_b is bed void fraction and u is superficial velocity.
[c] Pressure drop coefficient in Eq. (9).

For the sake of simplicity, but without loss of generality, we will consider as a case study the separation of the enantiomers of an allene compound, whose system parameters have been estimated experimentally and are reported in Table 1[11].

3.1. Detailed model equations

The models of the I-SMB process and of the conventional SMB process are obtained by combining single column models using proper boundary conditions and implementing proper port switching rules. The model equations of a chromatographic column described using the so-called equilibrium dispersive model for a binary system subject to a general adsorption isotherm given by $n_i^* = f_i(c_A, c_B)$ are [13–15]:

$$\epsilon^* \frac{\partial c_i}{\partial t} + (1-\epsilon^*)\frac{\partial n_i^*}{\partial t} + u\frac{\partial c_i}{\partial z} = \epsilon^* D_{ap,i}\frac{\partial^2 c_i}{\partial z^2} \quad (i = \mathrm{A,B}). \tag{14}$$

where t and z are time and space coordinates, u is the fluid superficial velocity, and the effects of axial dispersion, proportional to $D_{ax,i}$, and of the mass-transfer resistance, inversely proportional to $k_{s,i}a_v$, are lumped together in an effective dispersion term proportional to the apparent dispersion coefficient $D_{ap,i}$. The relationship between the actual parameters mentioned above and the apparent dispersion coefficient is given in the case of linear chromatography by the following form of the Van Deemter equation:

$$\mathrm{HETP}_i = \frac{2\epsilon_b D_{ax,i}}{u} + \frac{2u}{(1-\epsilon^*)H_i k_{s,i}a_v}\left(\frac{(1-\epsilon^*)H_i}{\epsilon^* + (1-\epsilon^*)H_i}\right)^2 = \frac{2\epsilon^* D_{ap,i}}{u}, \tag{15}$$

where ϵ_b is the interparticle bed void fraction. The Danckwerts boundary conditions are implemented at the inlet and outlet of each column as:

$$\epsilon^* D_{ap,i}\frac{\partial c_i}{\partial z}|_{z=0} = u(c_i|_{z=0} - c_i^{\mathrm{IN}}), \quad \frac{\partial c_i}{\partial z}|_{z=L} = 0. \tag{16}$$

Table 2
Operating conditions and purity performance of the simulated SMB and I-SMB runs; both units are operated in the 1-1-1-1 configuration; model parameters are reported in Table 1; the position of the operating points in the operating parameter plane is shown in Fig. 3.

Operating mode	Point	Flow rate ratio				t^* (s)	α	Flow rate (mL/min)				Purity (%)	
		m_1	m_2	m_3	m_4			Q_1	Q_2	Q_3	Q_4	Raffinate	Extract
SMB	P	3.82	1.96	2.88	1.33	41.1	–	7.43	4.94	6.16	4.08	97.6	99.5
	O	3.82	1.66	3.18	1.33	41.1	–	7.43	4.53	6.57	4.08	92.6	96.0
	N	3.82	1.36	3.48	1.33	41.1	–	7.43	4.12	6.98	4.08	84.6	85.5
I-SMB	P	3.82	1.96	2.88	1.33	41.1	0.28	12.04	3.08	7.49	5.65	99.9	100.0
	O	3.82	1.66	3.18	1.33	41.1	0.28	12.04	1.61	8.96	5.65	96.1	99.2
	N	3.82	1.36	3.48	1.33	41.1	0.28	12.04	0.14	10.43	5.65	84.4	85.8

where c_i^{IN} is the concentration of the inlet stream to the column. For the simulations, the model Eq. (14) with the conditions Eq. (16) are discretized using a first-order backward difference scheme and the system of ordinary differential equations (ODEs) thus obtained is solved numerically using a ODE solver based on backward differentiation. The model above is regarded as accurate enough to account for all the important features of multicolumn chromatographic processes.

3.2. Equilibrium theory of chromatography

For the purpose of SMB analysis and design the local equilibrium model of chromatography is effectively used. This is obtained from Eq. (14) by setting the apparent dispersion coefficient equal to zero, thus yielding the following equations (one for each species) in the case where the components to be separated are subject to the linear isotherm $n_i^* = H_i c_i$:

$$[\epsilon^* + (1-\epsilon^*)H_i]\frac{\partial c_i}{\partial t} + u\frac{\partial c_i}{\partial z} = 0. \tag{17}$$

Solving the equilibrium theory equations using the method of characteristics demonstrates that, for each species in solution, concentration levels propagate along the column at the concentration independent velocity given by the following equation [12]:

$$v_i = \frac{u}{\epsilon^* + (1-\epsilon^*)H_i}. \tag{18}$$

When applied to the different sections of the SMB unit this expression is fully consistent with that of Eq. (3) giving the retention time of species *i*.

3.3. Equilibrium theory cyclic steady-state

The cyclic steady-state performance of the conventional SMB and of the I-SMB processes (in a 1-1-1-1 configuration) will be determined using the equilibrium theory model first and then using the detailed model. The three operating points N, O and P in Fig. 3 will be considered for the equilibrium theory analysis, the first and the third being outside and inside the complete separation region, respectively, and the second being on its vertex. The operating parameters in sections 1 and 4 are the same for all operating points, as shown in Fig. 3 and reported in Table 2 where together with the flow rate ratios also the switch time, step ratio, flow rates and product purities (as cal-

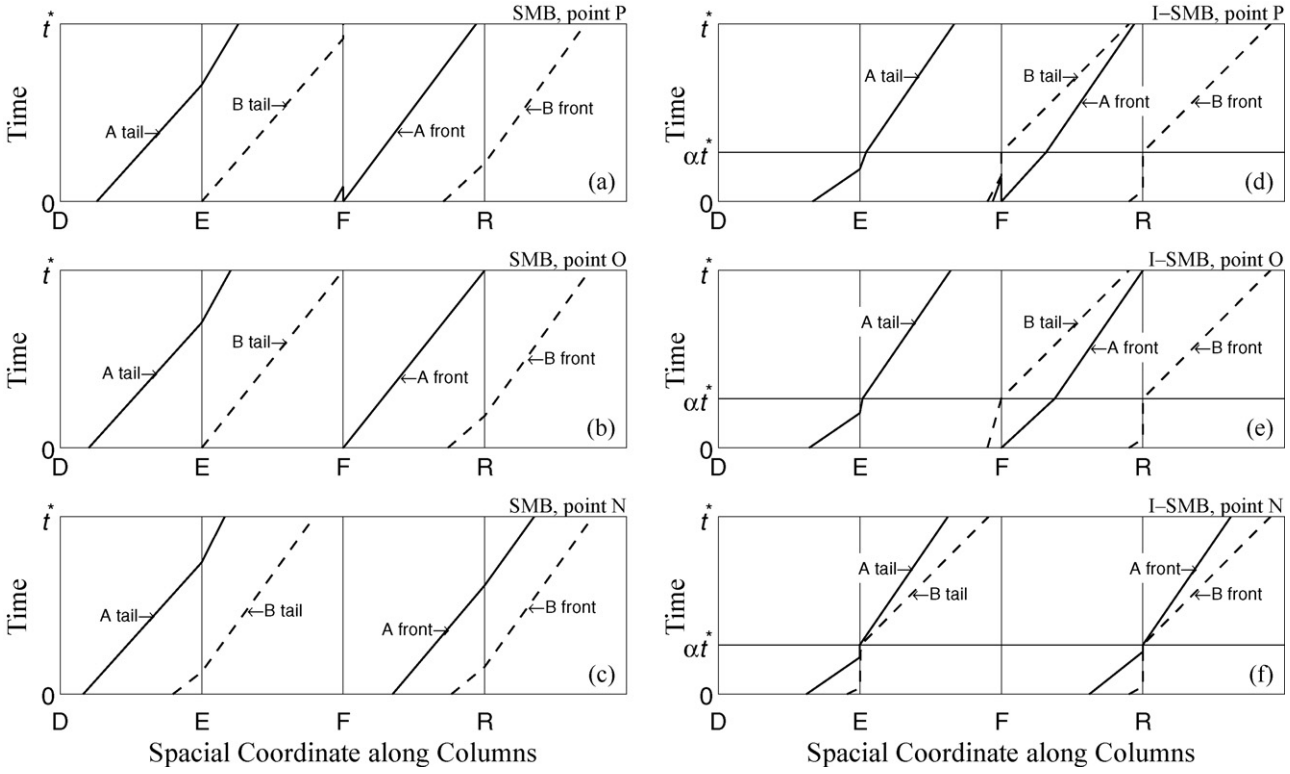

Fig. 4. Equilibrium theory cyclic steady-state solutions of conventional 4-column SMB and I-SMB processes. (a) Conventional SMB, point P. (b) Conventional SMB, point O. (c) Conventional SMB, point N. (d) I-SMB, point P. (e) I-SMB, point O. (f) I-SMB, point N.

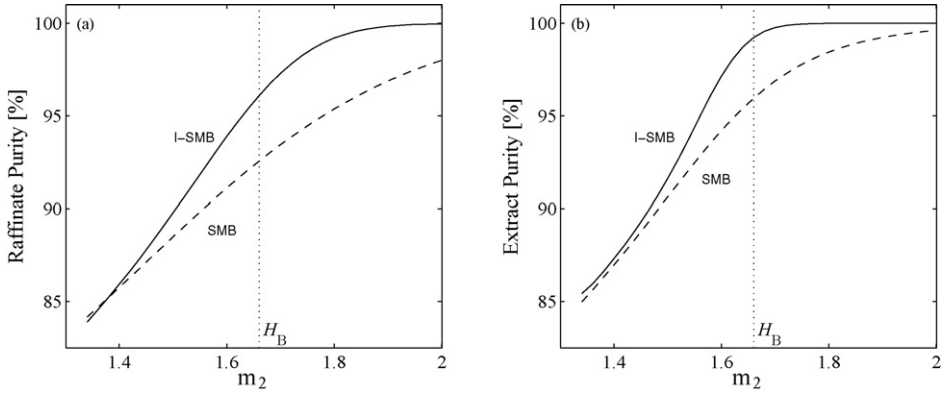

Fig. 5. Product purities for the conventional SMB and the I-SMB processes calculated using the equilibrium dispersive model for the operating points on the segment connecting points N and P in Fig. 3(a) raffinate; (b) extract.

culated through detailed simulations, as discussed below) are reported.

3.3.1. Conventional SMB

Let us consider Fig. 4(b), which refers to the conventional SMB operation at the operating point O, i.e. at the vertex of the complete separation region in the m_2-m_3 plane. This is a space-time diagram representing the SMB cyclic steady-state behavior, where the fluid flow is from left to right. The four SMB columns (numbered from left to right) are considered during the time interval t^*; the inlet and outlet ports are indicated underneath the horizontal axis, and will be shifted by one column to the right at the end of the switching period.

The solid and the dashed lines represent the trailing (tail) and the leading (front) edges of the more and less retained component, respectively, and delimit the area in the physical plane where the relevant component is present. Between B's trailing edge and A's leading edge both components are present. Thus, the position of the leading edge of component A indicates that there is no A in column 3 at the beginning of the time interval; that it enters column 3 because it is in the feed and in the outlet of column 2; and that component A reaches the end of column 3 (corresponding to the raffinate port) exactly at the end of the time interval, when upon port switch the leading edge of A finds itself again at the beginning of the new column 3, thus avoiding raffinate pollution by A. Likewise, since the trailing edge of B remains in column 2 and does not reach column 1, there is no extract pollution by B. The slopes of the A and B fronts are the reciprocal of their propagation velocity as given by Eq. (18) and calculated using the column superficial velocity, i.e. Q_j/S, hence they differ for A and B and from column to column. Cyclic steady-state is attained when the species profile at the end of the time interval is the same as the profile at the beginning, but shifted by one column to the right. This requirement is fulfilled by the diagram in Fig. 4(b) (as well as by the other five diagrams in the same figure).

From Eq. (2), the position of A's leading front in column 3 and of B's trailing front in column 2 implies that $t^{r}_{A,3} = t^*$ and that $t^{r}_{B,2} = t^*$, respectively. From Eq. (6) applied to the conventional SMB, these are equivalent to $m_3 = H_A$ and $m_2 = H_B$, i.e. the vertex of the complete separation region in Fig. 3. These equalities are replaced by inequalities in the other two columns, since flow rates are such that A is faster and B is slower in columns 1 and 4, respectively, i.e. $t^{r}_{A,1} < t^*$ and $t^{r}_{B,4} > t^*$, and $m_1 > H_A$ and $m_4 < H_B$. As a consequence, component A is completely eluted from column 1 at the end of the time interval illustrated in Fig. 4(b), whereas component B is absent from column 4 at the beginning of the time interval.

Let us now consider Fig. 4(a) that refers to the operating point P within the complete separation region. It is apparent that $t^{r}_{A,3} > t^*$ and that $t^{r}_{B,2} < t^*$, and thus also in this case extract and raffinate are not polluted. However, there is a certain clearing, i.e. separation (in space) between the position reached by the leading front of A at the end of the time period between two port switches and the raffinate port, which is missing in the case of Fig. 4(b). In the latter case, any deviation from the equilibrium theory prediction, e.g. due to axial dispersion, causes pollution of the raffinate. The same

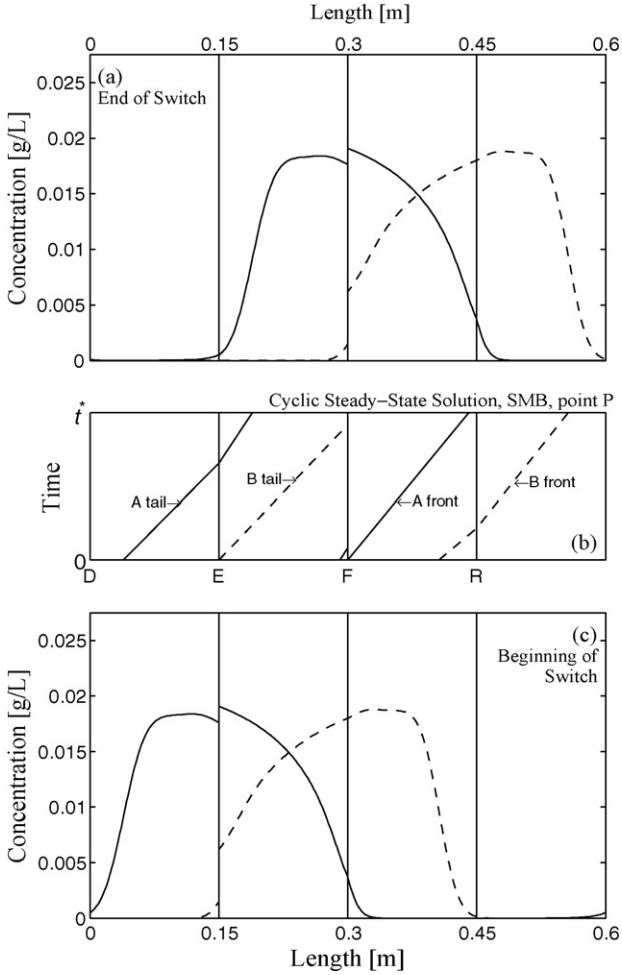

Fig. 6. Conventional SMB operation at operating point P. (a) Steady-state fluid phase concentration profile at the end of the switch. (b) Equilibrium theory cyclic steady-state solution. (c) Steady-state fluid phase concentration profile at the beginning of the switch. Mobile phase concentration profiles are calculated for a total feed concentration of 0.05 g/L.

situation occurs for component B, whose trailing edge in Fig. 4(a) reaches the end of column 2 earlier than when ports are switched and the extract port is moved to the end of column 2 (clearing in time, measured on the vertical axis at the position of the feed port), whereas in Fig. 4(b) any deviation from ideality would cause extract pollution.

Finally, Fig. 4(c) refers to the operating point N outside the complete separation region. Since $t^{r}_{A,3} < t^{*}$ and $t^{r}_{B,2} > t^{*}$, the cyclic steady-state shows that both extract and raffinate are polluted.

3.3.2. I-SMB

Figs. 4(d), (e) and (f) refer to the I-SMB operation at points P, O and N in the m_2–m_3 plane. In the first sub-interval (step I) the slope of the fronts differ for the two components in the same column because of the different Henry's constants, and for the same component in different columns because of the different flow rates. Fronts do not propagate into column 4, because there is no flow in that column during step I. In the second sub-interval (step II), fronts of the same species have the same slope in all columns because the flow rate is the same along the I-SMB unit in step II.

Let us now consider Fig. 4(e), which refers to the operation at the vertex of the complete separation region. As in Fig. 4(b), A's leading edge connects the feed port at the beginning of the time interval to the raffinate port at its end, which is the phenomenological manifestation of the optimal condition $m_3 = H_A$. However, A's leading edge is made of two segments of different slopes, and the clearing in space between it and the raffinate port is the one observed at the end of step I, as no raffinate is withdrawn during step II. Such clearing is much larger than that observed in the case of the conventional SMB operated at point P (see Fig. 4(a)), i.e. well within the complete separation region. B's trailing edge occupies a small portion of column 2 during step I and a large portion of column 3 during step II. As a consequence, the clearing in time between B's trailing edge and the position where the extract port is moved at the end of step II is very large, corresponding to more than half of t^{*}. Overall, A's leading edge and B's trailing edge are very close, i.e. much closer than in the SMB operation under the same conditions (Fig. 4(b)).

This is the key result of our analysis. At the vertex of the complete separation region the positions of the components' fronts in the I-SMB are such that, contrary to the case of the conventional SMB process, the effect of any small deviation from the ideal equilibrium theory behavior, due to axial dispersion or mass transfer resistance, can be tolerated by the unit without spoiling the products' purities.

This effect is also evident in the case of the operating point P, within the complete separation region, as illustrated in Fig. 4(d). Under the operating conditions of point N, outside the complete separation region, B's trailing edge and A's leading edge are moved backwards toward column 2 and forward toward column 4, respectively, as shown in Fig. 4(f). Considering that products are collected only during step I, it can be readily seen that the degree of products' pollution in Figs. 4(c) and (f) is very similar.

3.4. Detailed simulations of the cyclic steady-state

All results obtained using equilibrium theory in Section 3.3 are confirmed by analyzing the SMB and I-SMB cyclic steady-state using the equilibrium dispersive model defined in Section 3.1. The product purities calculated for a number of operating points along the segment in the m_2–m_3 plane connecting the operating points N, O and P in Fig. 3 are plotted as a function of a coordinate along the segment, namely m_2, in Fig. 5. The same purities in the operating points N, O and P are reported in Table 2. Note that the same values of t^{*} and α apply for all points along the N to P segment. It can be readily observed that the product purities drop as m_2 decreases in the case of the conventional SMB earlier than in the case of the I-SMB. More specifically in the case of I-SMB point P achieves indeed complete separation, whereas point O, i.e. the theoretical optimal point, exhibits very high extract purity and rather high raffinate purity. As predicted, SMB purity performance is much worse in point O, and not as good in point P, although this should be in the complete separation region. Interestingly, and again as predicted, product purity is the same for SMB and I-SMB operated outside the complete separation region, i.e. point N. This result demonstrates that the I-SMB process achieves higher productivity than the conventional SMB, because for a given purity specification the I-SMB can be operated closer to the tip of the triangle than the SMB, hence the feed flow rate and the productivity can be larger accordingly.

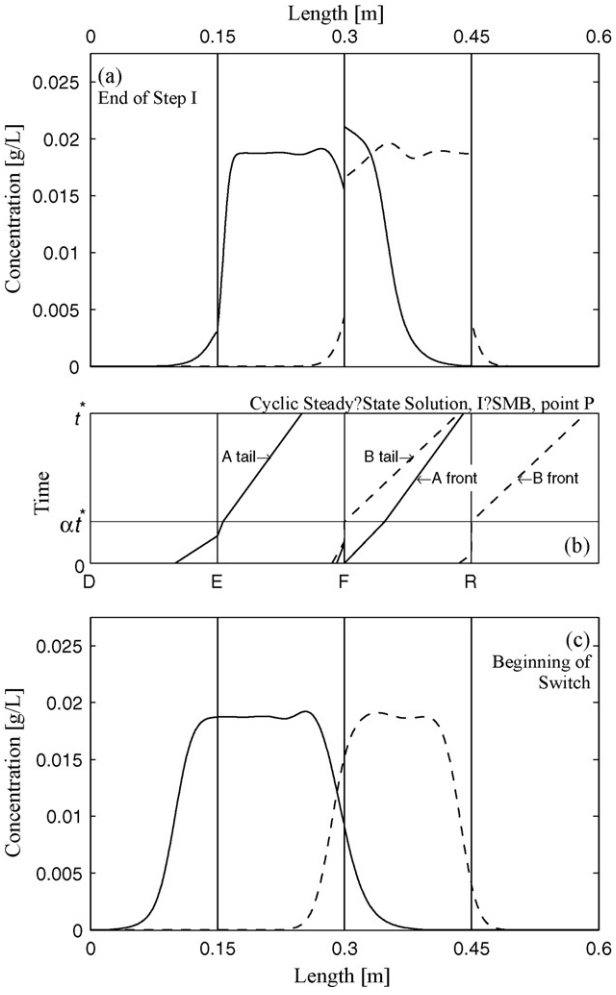

Fig. 7. I-SMB operation at operating point P. (a) Steady-state fluid phase concentration profile at the end of the switch. (b) Equilibrium theory cyclic steady-state solution. (c) Steady-state fluid phase concentration profile at the beginning of the switch. Mobile phase concentration profiles are calculated for a total feed concentration of 0.05 g/L.

Detailed simulations allow also analyzing the calculated concentration profiles in the fluid phase. These are shown in Figs. 6 and 7 for SMB and I-SMB operation, respectively, at point P, i.e. within the complete separation region. The cyclic steady diagrams of Figs. 4(a) and (d) are shown in the middle of the two figures; underneath them there are the concentration profiles at the beginning of the time interval, whereas above them there are those at the end of the switch time interval for the SMB and at the end of step I for the I-SMB, i.e. at the point in time where instantaneous product pollution is expected to be the most intense. It can readily be observed that in the conventional SMB case both the raf-

finate and the extract are polluted, albeit the latter only slightly. On the contrary, in the I-SMB case there is no such pollution and the feed mixture is indeed separated completely.

Detailed simulations confirm also that B's trailing edge and A's leading edge are much closer in the I-SMB unit of Fig. 7 than in the conventional SMB unit of Fig. 6, as predicted.

3.5. Conclusions

This paper presents the intermittent SMB technology, analyzes for the first time its behavior, and demonstrates why and how it has the potential to outperform the conventional SMB process. Such proof is based on the equilibrium theory of chromatography and is supported by detailed simulations. The impact of partial feed and withdrawal operations on the SMB performance has been discussed in previous publications [16–18]. Nevertheless, we believe that the I-SMB technology is simpler to implement, from both a theoretical and a practical point of view, and more effective. We are planning to substantiate this statement with future work that addresses systems subject to nonlinear adsorption isotherms and I-SMB optimization, as well as the experimental validation of all the theoretical results. We believe that the deployment of the I-SMB technology for difficult separations, such as that of the enantiomers of a chiral compound in the case of low selectivity, can be a major breakthrough in preparative multi-column chromatography.

References

[1] G. Paredes, M. Mazzotti, J. Chromatogr. A 1142 (2007) 56.
[2] A. Rajendran, G. Paredes, M. Mazzotti, J. Chromatogr. A 1216 (2009) 709.
[3] O. Ludemann-Hombourger, R.M. Nicoud, M. Bailly, Sep. Sci. Technol. 35 (2000) 1829.
[4] H. Schramm, A. Kienle, M. Kaspereit, A. Seidel-Morgenstern, Chem. Eng. Sci. 58 (2003) 5217.
[5] Z. Zhang, M. Mazzotti, M. Morbidelli, J. Chromatogr. A 1006 (2003) 87.
[6] L.C. Kessler, A. Seidel-Morgenstern, J. Chromatogr. A 1207 (2008) 55.
[7] M. Tanimura, M. Tamura, T. Teshima, Japanese Patent JP-B-H07–046097, 1995.
[8] G. Storti, M. Mazzotti, M. Morbidelli, S. Carrà, AIChE J. 39 (1993) 471.
[9] M. Mazzotti, G. Storti, M. Morbidelli, J. Chromatogr. A 769 (1997) 3.
[10] C. Migliorini, M. Mazzotti, M. Morbidelli, AIChE J. 45 (1999) 1411.
[11] S. Katsuo, C. Langel, P. Schanen, M. Mazzotti, J. Chromatogr. A 1216 (2009) 1084.
[12] H.-K. Rhee, R. Aris, N.R. Amundson, First-Order Partial Differential Equations, vol. 1: Theory and Application of Single Equations, Dover, New York, 2001.
[13] C. Migliorini, A. Gentilini, M. Mazzotti, M. Morbidelli, Ind. Eng. Chem. Res. 38 (1999) 2400.
[14] G. Guiochon, J. Chromatogr. A 965 (2002) 129.
[15] G. Guiochon, A. Felinger, D.G. Shirazi, A.M. Katti, Fundamentals of Preparative and Nonlinear Chromatography, 2nd Edition, Academic Press, New York, 2006.
[16] Y.-S. Bae, C.-H. Lee, J. Chromatogr. A 1122 (2006) 161.
[17] Y. Zang, P.C. Wankat, Ind. Eng. Chem. Res. 41 (2002) 2504.
[18] Y. Zang, P.C. Wankat, Ind. Eng. Chem. Res. 41 (2002) 5283.